Zygote

cambridge.org/zyg

All that glitters is not gold: a stereological study of human donor oocytes

Tânia Santos[1,2], Ana S. Pires-Luís[3,4], Ângela Alves[1,5], Elsa Oliveira[1,5], Carla Leal[5,6], Mónica Fernandes[5,6], Emídio Vale-Fernandes[5,6], Márcia Barreiro[5,6], Ana-Margarida Calado[2], Rosália Sá[1,5] and Mário Sousa[1,5]

[1]Laboratory of Cell Biology, Department of Microscopy, ICBAS-School of Medicine and Biomedical Sciences, University of Porto, Rua Jorge Viterbo Ferreira, 228, 4050–313 Porto, Portugal; [2]Department of Veterinarian Science, School of Veterinary and Agricultural Sciences (ECAV), CECAV – Interdisciplinary Research Center in Animal Health, Associated Laboratory for Animal and Veterinary Science (AL4AnimalS), University of Trás-os-Montes e Alto Douro (UTAD), Quinta de Prados, 5000–801 Vila Real, Portugal; [3]Department of Pathology, Centro Hospitalar de Vila Nova de Gaia/Espinho, Unidade 1, Rua Conceição Fernandes 1079, 4434–502, Vila Nova de Gaia, Portugal; [4]Laboratory of Histology and Embryology, Department of Microscopy, ICBAS-School of Medicine and Biomedical Sciences, University of Porto; [5]UMIB-Unit for Multidisciplinary Research in Biomedicine/ITR-Laboratory for Integrative and Translational Research in Population Health, University of Porto, Porto, Portugal and [6]Centro de Procriação Medicamente Assistida (CPMA), Centro Materno-Infantil do Norte (CMIN) Albino Aroso, Centro Hospitalar do Porto (CHUPorto), Largo da Maternidade de Júlio Dinis 45, 4050–651 Porto, Portugal

Research Article

Cite this article: Santos T *et al*. (2023) All that glitters is not gold: a stereological study of human donor oocytes. *Zygote*. **31**: 253–265. doi: 10.1017/S0967199423000114

Received: 8 August 2022
Accepted: 16 February 2023
First published online: 20 March 2023

Keywords:
Human donor oocytes; Human oocytes; Oocyte organelle distribution; Stereology; Ultrastructure

Author for correspondence:
Mário Sousa. Laboratory of Cell Biology (Director), Department of Microscopy, ICBAS-School of Medicine and Biomedical Sciences, University of Porto, Rua Jorge Viterbo Ferreira, 228, 4050–313 Porto, Portugal.
Tel: +91 9974476.
E-mail: msousa@icbas.up.pt

This paper has been updated since initial publication. A correction notice has been published detailing the change.

Summary

Here we report a quantitative analysis of human metaphase II (MII) oocytes from a 22-year-old oocyte donor, retrieved after ovarian-controlled hyperstimulation. Five surplus donor oocytes were processed for transmission electron microscopy (TEM), and a stereological analysis was used to quantify the distribution of organelles, using the point-counting technique with an adequate stereological grid. Comparisons between means of the relative volumes (Vv) occupied by organelles in the three oocyte regions, cortex (C), subcortex (SC) and inner cytoplasm (IC), followed the Kruskal–Wallis test and Mann–Whitney *U*-test with Bonferroni correction. Life cell imaging and TEM analysis confirmed donor oocyte nuclear maturity. Results showed that the most abundant organelles were smooth endoplasmic reticulum (SER) elements (26.8%) and mitochondria (5.49%). Significant differences between oocyte regions were found for lysosomes ($P = 0.003$), cortical vesicles ($P = 0.002$) and large SER vesicles ($P = 0.009$). These results were quantitatively compared with previous results using prophase I (GV) and metaphase I (MI) immature oocytes. In donor MII oocytes there was a normal presence of cortical vesicles, SER tubules, SER small, medium and large vesicles, lysosomes and mitochondria. However, donor MII oocytes displayed signs of cytoplasmic immaturity, namely the presence of dictyosomes, present in GV oocytes and rare in MI oocytes, of SER very large vesicles, characteristic of GV oocytes, and the rarity of SER tubular aggregates. Results therefore indicate that the criterion of nuclear maturity used for donor oocyte selection does not always correspond to cytoplasmic maturity, which can partially explain implantation failures with the use of donor oocytes.

Introduction

According to data published by the World Health Organization, infertility is a condition that affects ~48 million couples and 186 million individuals worldwide (WHO, 2020). Female infertility is responsible for approximately half of the cases, with ovarian ageing being a current societal dilemma (Walker and Tobler, 2022).

Oocyte quality is a critical component in overall fertility, as oocyte competence is critical for normal fertilization, embryonic development, implantation and full pregnancy (Conti and Franciosi, 2018; Sirait *et al*., 2021). Oocyte competence is acquired during oogenesis, where the oocyte passes through a sequence of maturation changes involving both nuclear and cytoplasmic domains (Arroyo *et al*., 2020). Nuclear maturation includes a cascade of events culminated by the pre-ovulatory peak of luteinizing hormone (LH), which allows the oocyte to resume meiosis and ovulate (Sánchez and Smitz, 2012). This process is characterized by nuclear envelope breakdown (GVBD: germinal vesicle breakdown) in prophase I oocytes (GV oocytes), followed by the condensation and alignment of chromosomes in a metaphase plate-I (MI oocytes). MI oocytes then enter the first meiotic division, with extrusion of the first polar body (PB1), containing half of the chromosomes, and condensation and alignment of the other half of the chromosomes in a metaphase plate-II (MII oocytes), with oocytes remaining in an MII arrest until fertilization (Arroyo *et al*., 2020). Nuclear maturation must occur in coordination with cytoplasmic maturation (Eppig, 1996). Cytoplasmic maturation is characterized by the

accumulation of mRNA, proteins, substrates and nutrients (Watson, 2007; Richani and Gilchrist, 2018; Cornet-Bartolomé *et al.*, 2021), as well as by the remodelling of organelles and the cytoskeleton (Mao *et al.*, 2014; Coticchio *et al.*, 2015: Reader *et al.*, 2017), in an intimate cross-talk with the surrounding follicular cells (Dumesic *et al.*, 2015; May-Panloup *et al.*, 2016).

Although the objective in assisted reproductive treatments (ART), using controlled hormonal ovarian hyperstimulation, is to obtain a maximum number of MII oocytes, in ~10–15% of the cycles immature oocytes, GV and MI, are also retrieved (Ebner *et al.*, 2003; Pinto *et al.*, 2009; Braga *et al.*, 2020), and, in a lower percentage, oocytes may display cytoplasmic and extracytoplasmic dimorphisms (Rienzi *et al.*, 2011; Sá *et al.*, 2011; Braga *et al.*, 2013, 2020; Sousa *et al.*, 2015, 2016a; Stigliani *et al.*, 2018), due to maturation defects (Windt *et al.*, 2001; Tripathi *et al.*, 2010; Conti and Franciosi, 2018; Ozturk, 2020). Some immature oocytes may resume meiosis during *in vitro* culture, but show reduced developmental competence (Ebner *et al.*, 2003, 2006; Shu *et al.*, 2007; Azevedo *et al.*, 2014; De Vos *et al.*, 2021; Karavani *et al.*, 2021).

Oocyte competence can be evaluated through morphologic and molecular analyses. The ultrastructural morphology of human oocytes at different maturation stages was evaluated in oocytes obtained from ART cycles (Baca and Zamboni, 1967; Zamboni *et al.*, 1972; Sathananthan and Trounson, 1982, 2000; Sathananthan, 1985, 1994, 1997; 2003; 2013; Sundström *et al.*, 1985; Motta *et al.*, 1988, 2000; Familiari *et al.*, 2006; Sathananthan *et al.*, 2006; Morimoto, 2009; Nottola *et al.*, 2014). Qualitative morphological studies have also been recently conducted in donor oocytes (Trebichalská *et al.*, 2021). Molecular research involved the analysis of oocyte and cumulus cells transcriptome (Cillo *et al.*, 2007; Gasca *et al.*, 2007; Wells and Patrizio, 2008; Ouandaogo *et al.*, 2012; Coticchio *et al.*, 2017), proteome (Virant-Klun *et al.*, 2016; Shen *et al.*, 2017) and metabolome (Venturas *et al.*, 2021), or zona pellucida gene mRNA expression (Canosa *et al.*, 2017), with development of oocyte quality markers (Sirait *et al.*, 2021).

Despite the importance of descriptive morphological studies, the qualitative evaluation of oocyte morphological characteristics can be incomplete or erroneous. As knowledge of the real morphology of the human oocyte is critical for the clinical development of new methods of cryopreservation and *in vitro* maturation, Pires-Luís *et al.* (2016) and Coelho *et al.* (2020) conducted pioneer quantitative studies with a stereological approach in GV and MI oocytes, respectively. In these studies, the relative volumes of the different organelles were measured and the distribution of organelles in the different regions of the oocyte, cortex, subcortex and inner cytoplasm (IC), were evaluated.

At this time, the use of donor oocytes showed an exponential increase due to the large improvements in the cryopreservation technique and luteal phase endometrium preparation (Walker and Tobler, 2022). Although with the use of donor oocytes live birth rates are high, there is still a place for implantation failures. This has been attributable to recipient uterine conditions or partner male factors [European IVF-Monitoring Consortium (EIM) for the European Society of Human Reproduction and Embryology (ESHRE), 2021; Sciorio *et al.*, 2021; Williams *et al.*, 2022], with the competence of donor oocytes being admitted to be optimized.

To our knowledge, this ultrastructural study is the first for donor MII oocytes using a stereological approach, in which we intended to quantify the spatial distribution of organelles. Surprisingly, we found a set of donor oocytes showing nuclear maturity but cytoplasmic immaturity. The results of the present report therefore provide evidence that even donor oocytes can show impaired competence.

Materials and methods

Ethical approval

Ethical guidelines were followed when conducting the research. According to the National Law on Medically Assisted Procreation (Law 32/2006) and the National Council for Medically Assisted Procreation guidelines (CNPMA, 2018), the use of clinical databases and surplus gametes for research may be used under strict individual anonymity and after patient written informed consent. Surplus donor oocytes were used after patients signed an informed consent agreeing to share their own gamete samples for the present study. The present laboratory experiments were executed under the Joint Ethics Committee of the Hospital and University, CHUP/ICBAS approval number 2019/CE/P017 (266/CETI/ ICBAS). This work did not involve human or animal experiments and therefore the provisions of the Declaration of Helsinki as revised in Tokyo 2004 do not apply.

Patients

This research was performed on five MII oocytes recovered from a 22-year-old oocyte donor after controlled ovarian stimulation during a donation programme performed at the Centro de Procriação Medicamente Assistida (CPMA), Centro Materno-Infantil do Norte (CMIN) Albino Aroso, Centro Hospitalar do Porto (CHUPorto), which is the National Gamete Bank.

Ovarian-controlled hyperstimulation

The oocyte donor underwent controlled ovarian hyperstimulation with a gonadotropin-releasing hormone antagonist protocol (GnRH; MSD, Hertfordshire, UK). Recombinant follicle-stimulating hormone (rFSH; Teva Biotech, Germany) was used for ovarian stimulation. A GnRH agonist (0.2 mg triptorelin; Ipsen Pharma Biotech, Signes, France) was administrated for triggering oocyte maturation, 36 h before follicular puncture (Huirne *et al.*, 2007; Pinto *et al.*, 2009).

Gamete and embryo handling

Procedures were performed on a K-Systems laminar flow chamber with a thermal base at 37°C (Cooper Surgical, Malöv, Denmark). Cumulus–oocyte complexes (COC) were collected in 1-well culture dishes (Falcon, Corning, New York, NY, USA) with SynVitro Flush medium (without heparin; Origio, Malöv, Denmark) and their handling and culture were performed under paraffin oil (Ovoil-100, Vitrolife, Frölunda, Sweden). After collection, COCs were washed and then cultured in Sequential Fert medium (Origio) in an Esco incubator (MRI-6A10, EscoMedical, Singapore, Singapore) (37°C, 5% O_2, 6% CO_2, 89% N_2) for 2 h. After denudation with recombinant hyaluronidase (ICSI Cumulase, Origio), oocytes were transferred to 4-well culture dishes (Nunc, Thermo Scientific, Denmark) with Sequential Fert medium (Origio) and processed for transmission electron microscopy (TEM). The remaining donor oocytes were vitrified under the National Gamete Bank programme according to Kitazato methodology (Kitazato Corporation, Japan).

https://doi.org/10.1017/S0967199423000114 Published online by Cambridge University Press

Transmission electron microscopy

Oocytes were fixed in Karnovsky solution (2.5% glutaraldehyde, 4% paraformaldehyde, 0.15 M sodium cacodylate buffer) (Sigma-Aldrich, St. Louis, USA; Merck, Darmstadt, Germany) at room temperature for 30 min, followed by 2 h at 4°C. After washing in 0.15 M sodium cacodylate buffer, pH 7.3 (Merck) for 2 h at 4° C, oocytes were post-fixed with 2% osmium tetroxide (Merck) in buffer containing 0.8% potassium ferricyanide (Merck) for 2 h at 4° C, washed in a buffer for 10 min, serially dehydrated in ethanol (Panreac, Barcelona, Spain), equilibrated with propylene oxide (Merck), and embedded in Epon (Sigma). Semithin and ultrathin sections were cut using diamond knives (Diatome, Hatfield, Switzerland) in an LKB ultramicrotome (Leica Microsystems, Weltzlar, Germany). A random number table was used to select the initial cut, and then oocytes were serially sectioned and sampled every 10 µm. Ultrathin sections were collected on 100 mesh formvar carbon-coated copper grids (Taab, UK) and stained with 3% aqueous uranyl acetate for 20 min (BDH, Poole, UK) and Reynolds lead citrate for 10 min (Merck) at room temperature in a light-protected environment. Ultrathin sections were observed on a JEOL 100CXII transmission electron microscope (JEOL, Tokyo, Japan) at 60 kV (Sousa and Tesarik, 1994; El-Shafie *et al*., 2000).

Stereological and statistical analysis

Systematic sampling was performed on each microscope grid, with photographs taken at alternate TEM field spaces when more than 50% of the field was occupied by the oocyte cytoplasm. Images were taken at ×5300 magnification and printed at 20.2 cm × 20.2 cm. A classical manual stereological technique based on point counting with a suitable stereological grid was used. The grid was placed over the printed photographs and the number of grid points placed over each organelle was noted. The relative volume (Vv) of each organelle was obtained by applying the formula Vv (organelle, oocyte) = [number of dots (organelle)/number of dots (oocyte)] × 100 (%) (Weibel *et al*., 1966).

Organelles included in the present evaluation were: cortical vesicles (CV), mitochondria, dictyosomes, lysosomes, medium-sized vesicles containing granular materials (VZP), smooth endoplasmic reticulum (SER) small vesicles (SER-SV), SER medium vesicles (SER-MV), SER large vesicles (SER-LV), SER very large vesicles (SER-VLV), SER isolated tubules (SER-IT), SER tubular aggregates (aSERT), and total SER without VLV (SV, MV, LV, IT, aSERT).

Each oocyte was divided into three regions, from the oolemma up to the cell centre: cortex (5 µm), subcortex (5–10 µm), and IC (>10 µm) (Figure 2A). A stereological procedure was adopted, applying the formula Vv (organelle, cortex/subcortex/IC) = [number of points (organelle)/number of points (cortex/subcortex/IC)] × 100 (%) (Pires-Luís *et al*., 2016).

Statistical analysis was performed using Microsoft® Excel 2022 and SPSS version 27.0 software (IBM Corp, Foster City, California, CA, USA). The results are presented as mean, standard error of the mean (SEM = standard deviation/$n^{1/2}$), and coefficient of variation (CVar = standard deviation/mean). Normal distribution was tested using the Kolmogorov–Smirnov test. The samples did not follow a normal distribution, and therefore non-parametric tests were used. To compare the means of Vv (organelle, oocyte), Vv (organelle, cortex), Vv (organelle, subcortex) and Vv (organelle, IC) the Kruskal–Wallis test and the Mann–Whitney *U*-test with Bonferroni correction were used. The level of statistical significance was set at $P < 0.05$.

Results

When observed under the inverted microscope, live MII oocytes displayed a rounded shape and a uniform fine granular cytoplasm, being surrounded by a thick translucent zona pellucida (ZP) and separated from the ZP by a short and narrow perivitelline space, where the PB1 was located (Figure 1A). In semithin sections, the oocyte evidenced the same structures, being additionally evident microvilli, CV and large vesicles. The oocyte metaphase II plate was also discernible, being placed slightly away from the cortical region. The PB1 showed chromosomes and the characteristic organelles of the cortical ooplasm (Figure 1B,C).

At the ultrastructural level, the oocyte surface exhibited numerous microvilli (Figure 2A,B), and in the perivitelline space the PB1 evidenced chromosomes and cortical ooplasm characteristics, including CV (Figure 2B). In the ooplasm, rows of electron-dense CV were observed under the oolemma and as isolated vesicles in the oocyte subcortex (Figure 2A). The metaphase II plate was slightly displaced towards the upper IC (Figure 2C). Mitochondria, SER-IT, SER-SV, SER-MV (Figure 2A) and SER-LV (Figure 3A) were observed in all three regions of the oocyte. The SER-VLV were found in the IC of one oocyte (Figure 3B). The aSERT was observed in all oocyte regions and also in one oocyte (Figure 4A,B). The VZP were observed in the oocyte cortex of two oocytes (Figure 4C). Lysosomes were observed in the cortex and inner ooplasm (Figure 4D). Dictyosomes were observed in the subcortex and IC of two oocytes (Figure 4E). The oocyte surface contained numerous tiny coated vesicles (Figure 4F). Multivesicular bodies, annulate lamellae, rough endoplasmic reticulum cisternae, lipid droplets and polyribosomes were not observed.

The present stereological analysis was performed on 204 photographs, with 96 representations of the cortex, 96 of the subcortex and 176 of the IC. The following organelles were quantified: mitochondria, dictyosomes, lysosomes, CV, VZP and SER elements (SER-SV, SER-MV, SER-LV, SER-VLV, SER-IT and aSERT).

The most predominant organelles in the total oocyte (Table 1) were SER-SV (Vv 8.84%), SER-IT (Vv 7.16%) and mitochondria (Vv 5.49%). This was followed by SER-MV (Vv 2.01%), LV-SER (Vv 0.79%), aSERT (Vv 0.61%), lysosomes (Vv 0.33%), CV (Vv 0.31%), SER-VLV (Vv 0.30) and dictyosomes (Vv 0.01%).

The most common organelles per oocyte region were (Table 1): in the cortex, SER-SV (Vv 9.67%) followed by SER-IT (Vv 8.19%) and mitochondria (Vv 5.66%); in the subcortex, SER-SV (Vv 8.74%), SER-IT (Vv 7.22%) and mitochondria (Vv 5.79%); and in the IC, SER-SV(Vv 8.40%), SER-IT (Vv 7.2%) and mitochondria (Vv 5.33%).

The three oocyte regions were compared using the Kruskal–Wallis test (Table 2) and no significant differences were found for mitochondria ($P = 0.677$), dictyosomes ($P = 0.317$), SER-SV ($P = 0.677$), SER-MV ($P = 0.102$), SER-VLV ($P = 0.368$), SER-IT ($P = 0.336$) and aSERT ($P = 0.980$). Conversely, significant differences were found for lysosomes ($P = 0.003$), CV ($P = 0.002$), VZP ($P = 0.032$) and SER-LV ($P = 0.009$). Strict pairwise comparisons for the three regions using the Mann–Whitney *U*-test, Bonferroni corrected (Table 2), showed that there were significant differences in the Vv of CV between the three regions of oocytes ($P = 0.008$), lysosomes showed significant differences between cortex vs IC and subcortex vs IC ($P = 0.008$), and SER-LV between cortex vs IC ($P = 0.032$) and subcortex vs IC ($P = 0.008$).

https://doi.org/10.1017/S0967199423000114 Published online by Cambridge University Press

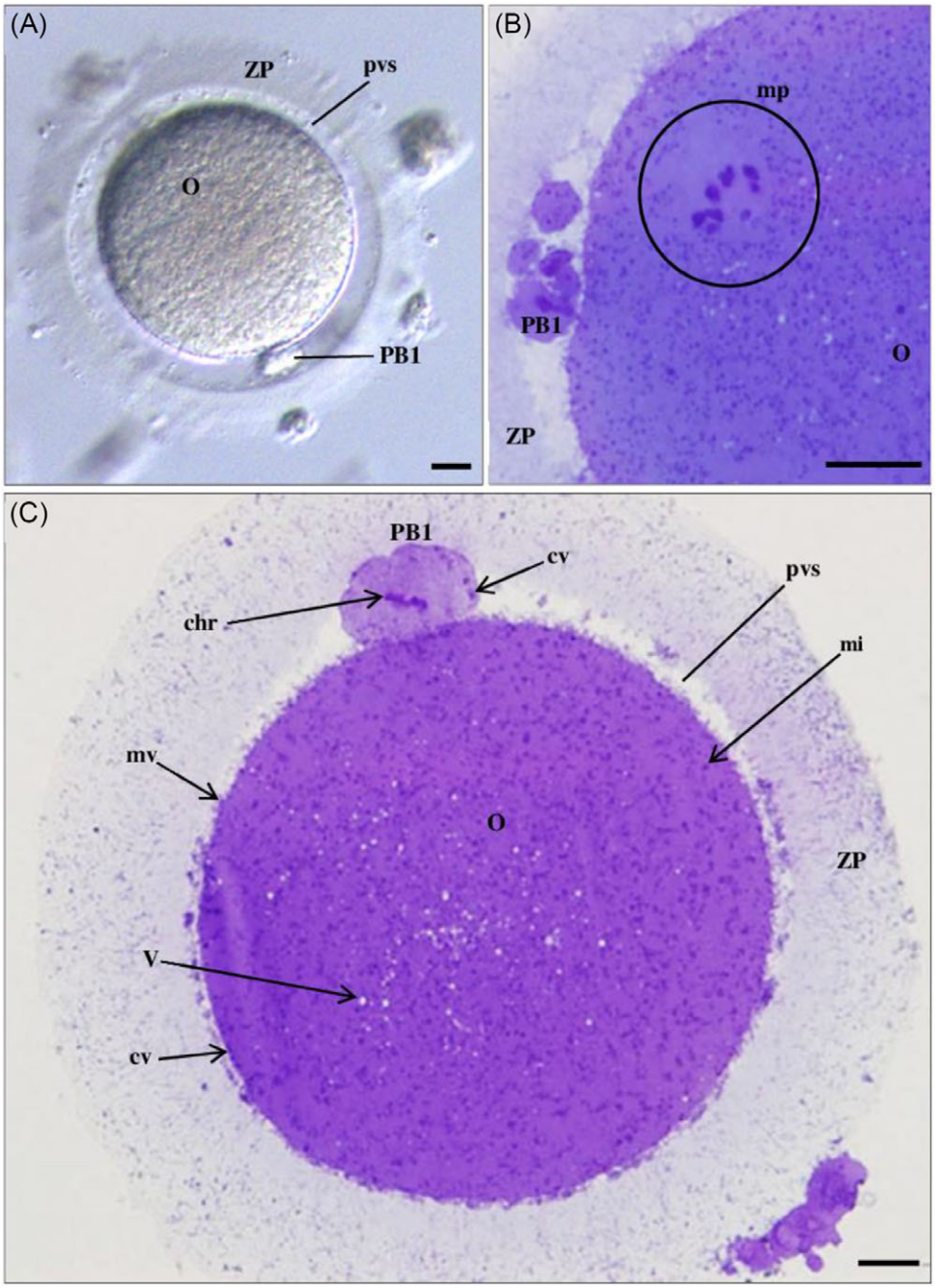

Figure 1. Metaphase II (MII) oocyte. (A) Live cell observed in the inverted microscope and (B, C) its correspondent semithin sections. The oocyte (O) was separated from the zona pellucida (ZP) by the perivitelline space (pvs), where resided the first polar body (PB1). In all cases, the ooplasm presented a homogeneous appearance. In semithin sections, all oocytes presented a metaphase place (mp) slightly dislocated towards the upper inner region. Chromosomes (chr) and cortical vesicles (cv) appeared evident in the PB1. The oocyte surface displayed numerous microvilli (mv). In the ooplasm, cortical vesicles (cv), mitochondria (mi) and large vesicles (V) can be observed. Bars: (A) 20 µm; (B, C) 10 µm.

Discussion

Donor oocytes are an important procedure in ART and in the last 30 years have become a more prevalent therapy of choice for many infertile patients (Yeh *et al.*, 2014). This study is based on the use of donor oocytes from a young woman by a recipient woman in ART procedures. Indications for donor oocytes include advanced reproductive age, diminished ovarian reserve, recurrent poor oocyte or embryo quality in IVF attempts, hypothalamic hypogonadism, and in some cases with the possibility of transmitting a genetic defect (Taylor, 2019; Sciorio *et al.*, 2021; Williams *et al.*, 2022). In oocyte donor cycles, in which ovarian hyperstimulation is used, it is necessary that nuclear and cytoplasmic maturation occurs in a coordinated manner to ensure optimal conditions for subsequent fertilization (Conti and Franciosi, 2018), but which does not always occur, resulting in nuclear, cytoplasmic or extracytoplasmic morphological abnormalities (Ten *et al.*, 2007; Setti *et al.*, 2021).

In previous works we presented the stereological analysis of human immature oocytes at the GV stage (Pires-Luís *et al.*, 2016) and MI stage (Coelho *et al.*, 2020). The present study was designed to apply the same technique to mature MII oocytes. To this end, we obtained 13 surplus donor MII oocytes, retrieved from six donors during oocyte donor programmes. In one case, the oocyte donor donated five oocytes for research, three cases gave two oocytes each, and two cases gave one oocyte each. In all cases, nuclear maturity was verified through inspection under an

https://doi.org/10.1017/S0967199423000114 Published online by Cambridge University Press

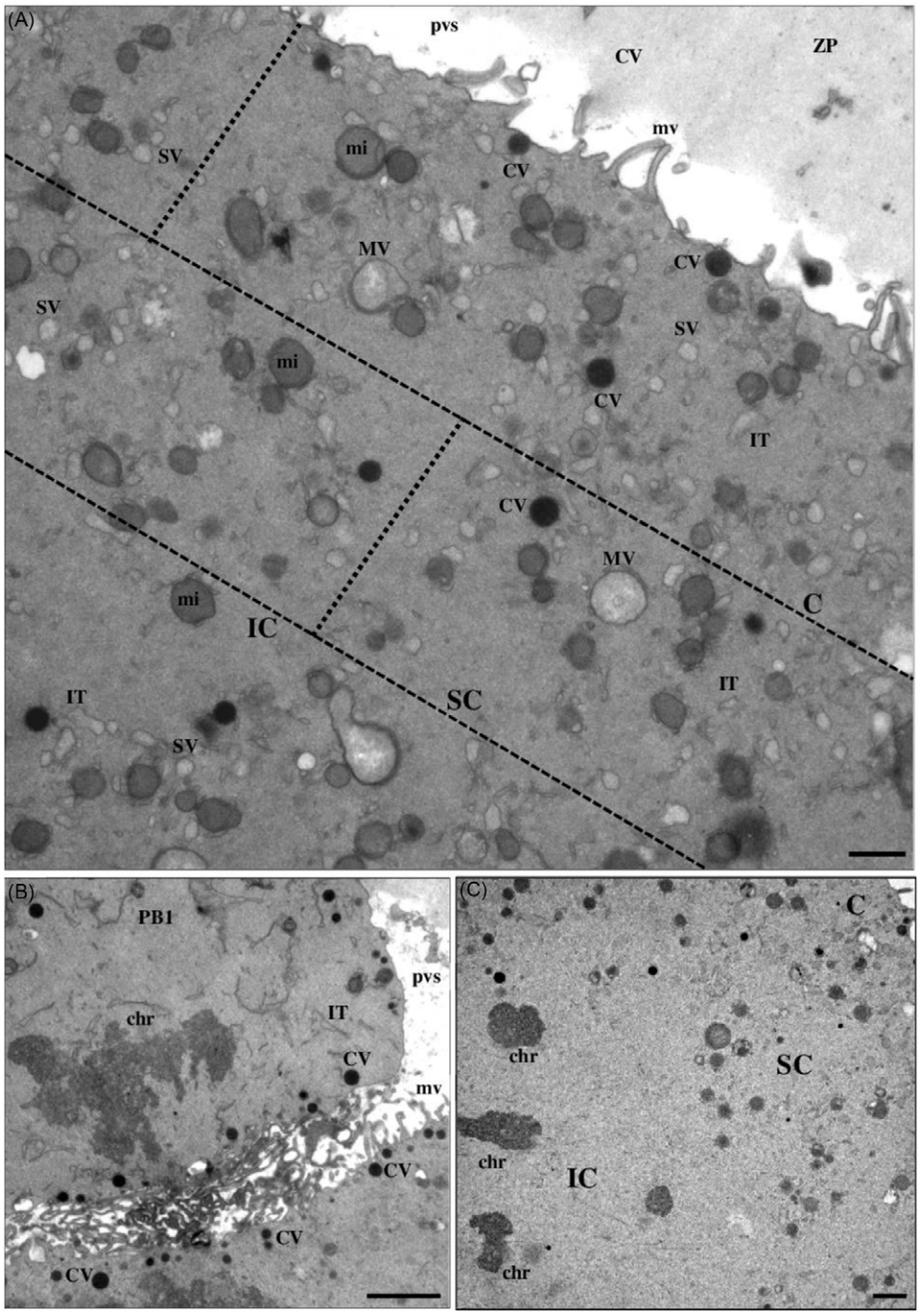

Figure 2. Ultrastructural images of metaphase II (MII) oocytes. (A, B) MII oocytes, showing the three regions, cortex (C), subcortex (SC) and inner (IC) cytoplasm. The oocyte surface is separated from the zona pellucida (ZP) by the perivitelline space (pvs), which contains oocyte microvilli (mv). Rows of cortical vesicles (cv) are observed under the oolemma and as isolated cortical vesicles in the cortex and subcortex regions. In the ooplasm mitochondria (mi) and smooth endoplasmic reticulum (SER) small (SV) and medium (MV) sized vesicles and isolated tubules (IT) can be observed. SER vesicles were barely associated with mitochondria. (B) The first polar body (PB1) exhibits chromosomes (chr) and cortical ooplasm elements, such as cortical vesicles (cv) and isolated SER tubules (IT). (C) The chromosomes (chr) of the oocyte metaphase II plate appeared slightly displaced towards the upper inner region. Bars: 1 μm.

inverted microscope (live oocytes), which confirmed the presence of the first polar body, and in semithin sections (fixed oocytes), which confirmed the presence of the first polar body and the metaphase II plate. Also, in all cases, cytoplasmic integrity was verified through inspection under an inverted microscope and in semithin sections, which confirmed the absence of intracytoplasmic or extracytoplasmic dimorphisms. We started with the donor that provided five oocytes, but TEM observations revealed cytoplasmic immaturity characteristics. Thereafter, we looked at the remaining MII oocytes from the donor to ensure their cytoplasmic maturity. However, all five MII oocytes revealed cytoplasmic immaturity, evidencing an unconformity between nuclear and cytoplasmic maturity. The current study focuses on the examination of these five oocytes obtained from a single donor.

Previous ultrastructural studies of mature MII oocytes showed the presence of PB1 in the perivitelline space, containing chromosomes and the organelles of the cortical ooplasm (Zamboni *et al.*, 1972; Sathananthan, 1994). An organized metaphase II plate could also be observed in the cortical/subcortical region near the PB1 (Zamboni *et al.*, 1972; Sathananthan, 2013). The oocyte surface presented numerous microvilli (Morimoto, 2009) and CV formed one or more layers next to the oolemma (Sathananthan and Trounson, 1982; Motta *et al.*, 1988), with some cortical regions presenting a higher density of CV than others (Sathananthan and

https://doi.org/10.1017/S0967199423000114 Published online by Cambridge University Press

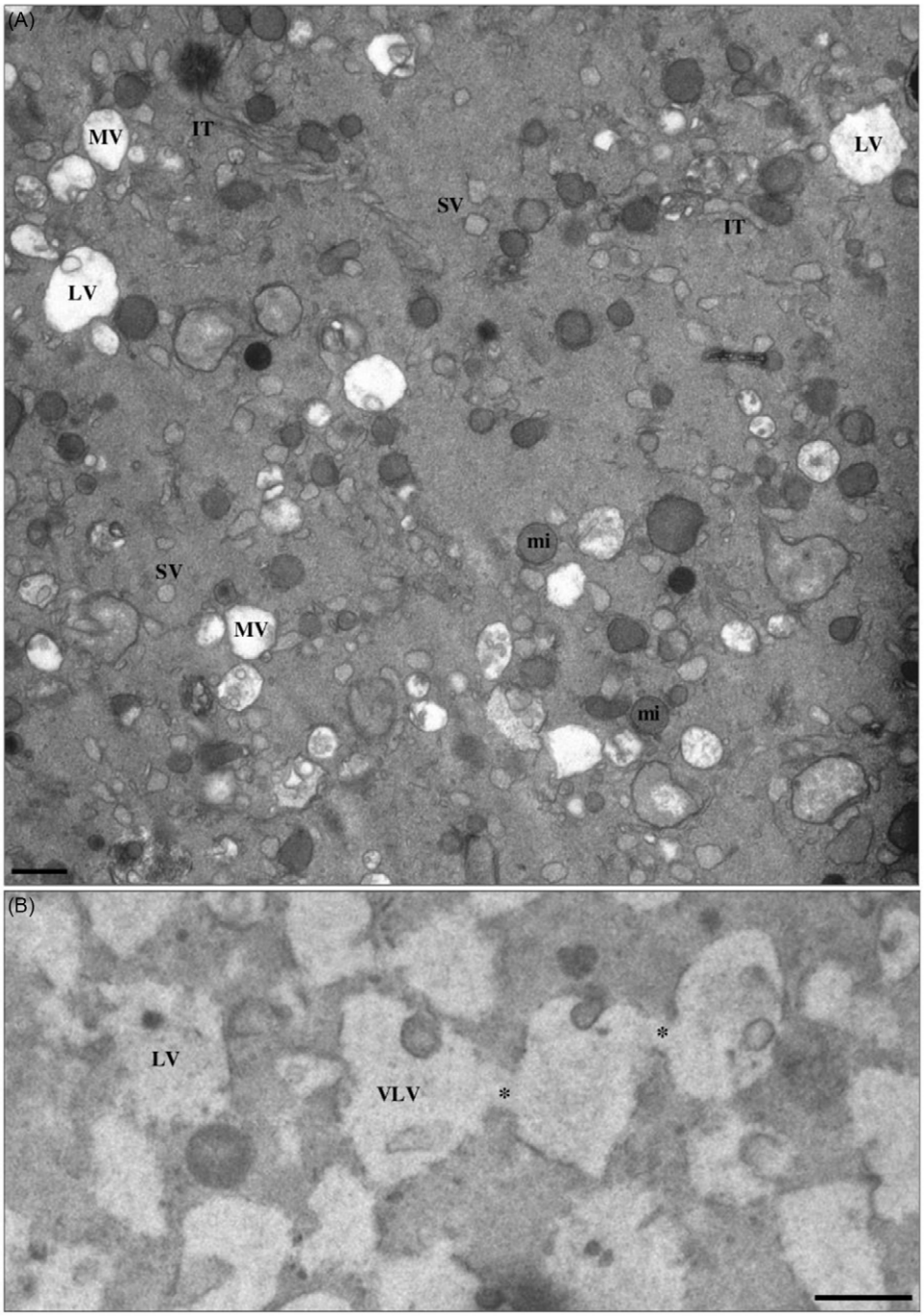

Figure 3. Ultrastructural images of metaphase II oocytes at the inner oocyte region. (A) In the inner cytoplasm mitochondria (mi) and smooth endoplasmic reticulum (SER) small (SV), medium (MV) and large (LV) sized vesicles and isolated tubules (IT) can be observed. Note that SER vesicles are barely associated with mitochondria. (B) The inner cytoplasm also presented SER very large vesicles (VLV), with their characteristic bridges (*).

Trounson, 1982; Sousa and Tesarik, 1994; El-Shafie *et al.*, 2000; Sousa *et al.*, 2016b). The oocyte cortex and subcortex were enriched in SER vesicles of various sizes, SER-IT and aSERT (Sousa and Tesarik, 1994; El-Shafie *et al.*, 2000; Sathananthan, 2013; Sousa *et al.*, 2016b). Mitochondria were described as evenly distributed, surrounding most SER vesicles and aSERT, and forming necklace-like complexes (Sundström *et al.*, 1985; Motta *et al.*, 1988, 2000; El-Shafie *et al.*, 2000; Sathananthan and Trounson, 2000; Morimoto, 2009; Nottola *et al.*, 2014; Sousa *et al.*, 2016b; Trebichalská *et al.*, 2021). Lysosomes were also described (Sathananthan, 2003; Trebichalská *et al.*, 2021), and dictyosomes (Sathananthan *et al.*, 2006; Nottola *et al.*, 2014) and annulate lamella (Sathananthan *et al.*, 2006) were rarely observed. Some organelles and cytoplasmic structures were not found in mature MII oocytes, such as rough endoplasmic reticulum and multivesicular bodies (Sundström *et al.*, 1985), polyribosomes and lipid droplets (Sathananthan, 1994), just as in donor oocytes (Trebichalská *et al.*, 2021).

We here describe the presence of cortical tiny coated vesicles, which were previously observed in GV and MI oocytes (Pires-Luís *et al.*, 2016; Coelho *et al.*, 2020), and in mature MII oocytes (El-Shafie *et al.*, 2000; Sousa *et al.*, 2016b), indicating exchanges of materials with the exterior by receptor-mediated endocytosis (Hinduja *et al.*, 1990; Pires-Luís *et al.*, 2016; Sousa *et al.*, 2016b; Coelho *et al.*, 2020).

Our present observations confirm those previous findings, but several characteristics of immaturity were also observed in the

https://doi.org/10.1017/S0967199423000114 Published online by Cambridge University Press

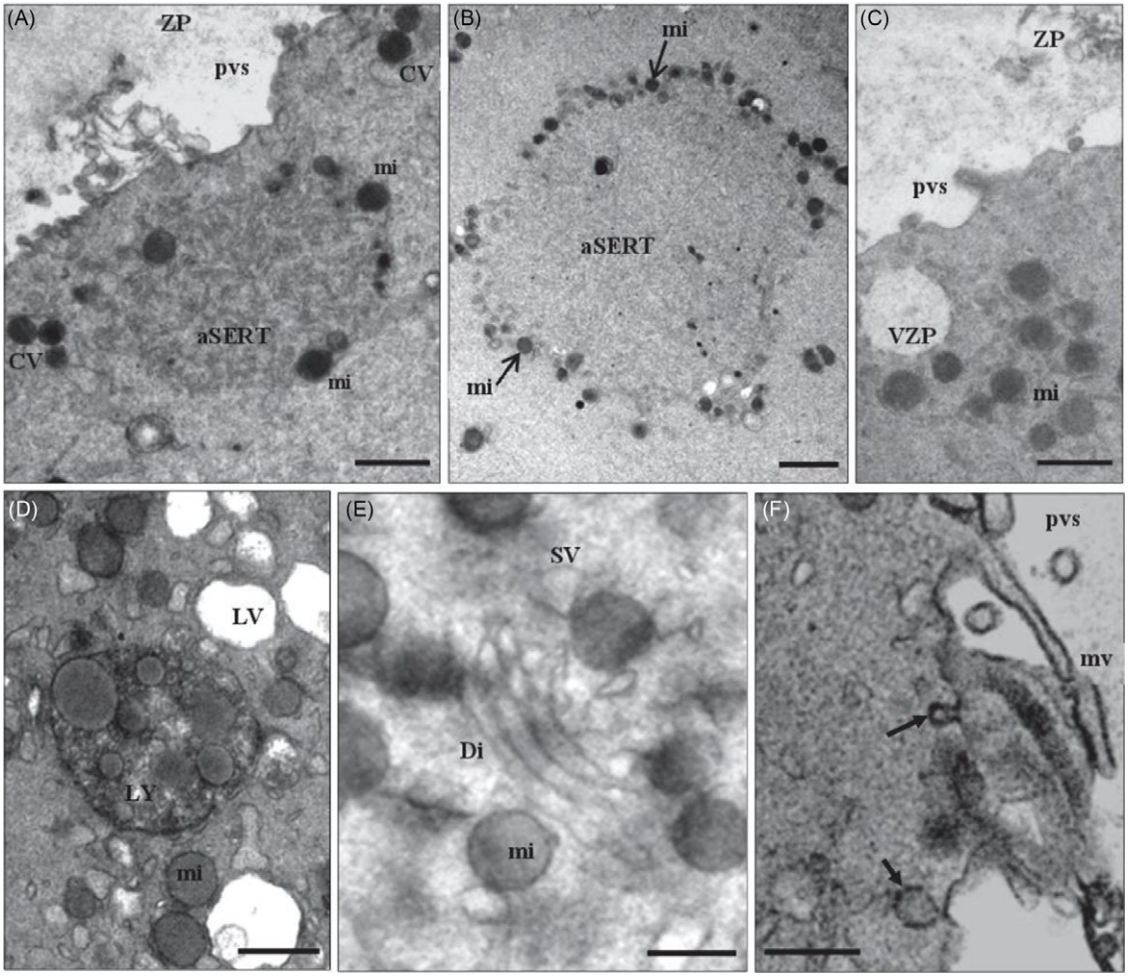

Figure 4. Ultrastructural images of metaphase II oocytes. (A, B) Aggregates of smooth endoplasmic reticulum tubules (aSERT) in cortical (A) and inner (B) oocyte regions, surrounded by mitochondria (mi). (C) Vesicles containing granular materials (VZP) in the oocyte cortical region. (D) Lysosome (LY) in the inner ooplasm. (E) Dictyosome (Di) in the inner ooplasm. (F) The oocyte surface showed numerous tiny coated vesicles (arrows). ZP: zona pellucida; pvs: perivitelline space; mv: microvilli; SV, LV: small (SV) and large (LV) smooth endoplasmic reticulum vesicles. Bars: (A, C, D) 1 μm; (B) 1 μm; (E, F) 0.5 μm.

ooplasm. These immature characteristics were the following: CV were observed in the oocyte cortex and subcortex, as in GV and MI oocytes (Pires-Luís *et al.*, 2016; Coelho *et al.*, 2020), being that they were expected to be only present in the cortical ooplasm; granular vesicles, suspected of containing ZP-like materials, were observed in the oocyte cortex, as in GV oocytes (Pires-Luís *et al.*, 2016), and although observed in only two oocytes (oocytes 2 and 3), it was expected they would not be found similarly to MI oocytes (Coelho *et al.*, 2020); dictyosomes were observed in the oocyte subcortex, as in GV oocytes (Pires-Luís *et al.*, 2016) and in the IC, as in GV and MI oocytes (Pires-Luís *et al.*, 2016; Coelho *et al.*, 2020), and although observed in only two oocytes (oocytes 1 and 3), they were expected to be not found, although there are two previous reports in mature MII oocytes that observed rare dictyosomes (Sathananthan *et al.*, 2006; Nottola *et al.*, 2014); SER-VLV were observed in the IC in only one oocyte (oocyte 4), but these are a GV characteristic (Pires-Luís *et al.*, 2016); aSERT were missing in oocytes 1–4, and the oocyte exhibiting aSERT (oocyte 5) presented this organelle in all three oocyte regions, as in MI oocytes (Coelho *et al.*, 2020). The aSERT in mature MII oocytes are limited to the oocyte cortex and subcortex, being critical for the oocyte to develop calcium oscillations at fertilization (Sousa *et al.*, 1996, 1997), without which the oocyte is not activated and no embryo development occurs (Dale *et al.*, 2010).

Therefore, all oocytes exhibited abnormal cortical vesicle positioning in the subcortex and all presented absence or abnormal positioning of aSERT. Additionally, in all cases, mitochondria appeared barely associated with SER-MV and SER-LV, and the metaphase II plate was slightly displaced from the cortical/subcortical region towards the IC. This renders the ooplasm of these donor MII oocytes immature.

By using a quantitative approach, when MII oocytes were compared in their different regions (Table 2), it was shown that there were no significant differences in the Vv of mitochondria among the three oocyte regions, corroborating what was reported in descriptive studies, in which a homogeneous distribution throughout the ooplasm was observed. Although mitochondria were described as the most predominant organelle in the ooplasm (Motta *et al.*, 1988, 2000; Sathananthan and Trounson, 2000; Trebichalská *et al.*, 2021), this was not observed in the present

https://doi.org/10.1017/S0967199423000114 Published online by Cambridge University Press

Table 1. Relative volume (Vv) of organelle per total MII oocyte and per MII oocyte regions: cortex, subcortex and inner cytoplasm

Organelle	Vv (organelle, oocyte) mean (%) +-SEM (Cvar)	Vv (organelle, cortex)	Vv (organelle, subcortex)	Vv (organelle, inner cytoplasm)
Mi	5.49 ± 0.30 (0.12)	5.66 ± 0.79 (0.313)	5.79 ± 0.48 (0.186)	5.33 ± 0.32 (0.135)
Di	0.01 ± 0.0085 (1.46)	0	0.01 ± 0.01 (2.24)	0.018 ± 0.013 (1.68)
Ly	0.33 ± 0.11(0.74)	0.03 ± 0.021 (1.50)	0	0.54 ± 0.18 (0.739)
CV	0.31 ± 0.057 (0.403)	1.29 ± 0.27 (0.462)	0.16 ± 0.05 (0.30)	0
VZP	0.02 ± 0.0097 (1.31)	0.084 ± 0.05 (1.35)	0	0
SV	8.84 ± 1.87(0.47)	9.67 ± 1.55 (0.359)	8.74 ± 1.92 (0.49)	8.40 ± 1.98 (0.517)
MV	2.01 ± 0.46 (0.51)	1.04 ± 0.46 (0.989)	0.74 ± 0.38 (1.14)	2.75 ± 0.67 (0.544)
LV	0.79 ± 0.38 (1.09)	0.12 ± 0.12 (2.24)	0.012 ± 0.012 (2.24)	1.27 ± 0.66 (1.17)
VLV	0.30 ± 0.29(2,236)	0	0	0.49 ± 0.49 (2.24)
IT	7.16 ± 0.69 (0.214)	8.19 ± 0.83(0.227)	7.22 ± 1.02 (0.316)	7.2 ± 0.58 (0.1798)
aSERT	0.61 ± 0.61 (2.24)	0.98 ± 0.98(2.24)	0.38 ± 0.38 (2.24)	0.44 ± 0.44 (2.24)
Total SER (without VLV)	26.8 ± 3.31 (0.276)	19.99 ± 2.17 (0.243)	17.1 ± 2.71 (0.355)	20.1 ± 1.46 (0.16)

Results presented as mean, SEM (standard error of the mean: standard deviation/$n^{1/2}$), and CVar (coefficient of variation: standard deviation/mean).
Mi: mitochondria; Di: dictyosomes; Ly: lysosomes; CV: cortical vesicles; VZP: vesicles containing zona pellucida-like material; SER: smooth endoplasmic reticulum; SV: SER small vesicles; MV: SER medium vesicles; LV: SER large vesicles; VLV: SER very large vesicles; IT: SER isolated tubules; aSERT: SER tubular aggregates.

study (Table 2), with quantitative analyses showing that the SER is the most predominant organelle (Table 1) (Mi Vv 5.49% vs total SER Vv 26.8%).

Using strict pairwise comparisons for the three oocyte regions and the Mann–Whitney *U*-test, Bonferroni corrected (Table 2), significant differences were observed for the following and the SER-LV presented a higher prevalence in the IC. This finding contradicts morphological study descriptions, in which lysosomes and SER-LV were seen to be distributed uniformly (Zamboni *et al.*, 1972; Sundström *et al.*, 1985; Motta *et al.*, 1988).

Applying a stereological analysis similar to that previously used in human immature oocytes, GV (Pires-Luís *et al.*, 2016) and MI (Coelho *et al.*, 2020), it was possible to compare quantitatively immature oocytes with the present studied MII oocytes.

Comparing GV with MII oocytes (Table 3), no significant differences were observed in the Vv of mitochondria, lysosomes, CV, VZP and SER-LV. For mitochondria, the Vv was lower in MII oocytes, except in the cortex, and was only significantly lower in the IC; for lysosomes and VZP, no significant differences in the Vv were found along all oocyte regions; in relation to CV, the Vv were similar in the cortex and subcortex; the significant difference observed in the IC were due to the absence of CV in that region of MII oocytes; for SER-LV, the Vv were similar but nevertheless higher in the cortex and IC of MII oocytes, and significantly lower in the subcortex of MII oocytes. Significant differences in all oocyte regions were observed in the Vv of dictyosomes, SER-SV, SER-MV, SER-VLV, SER-IT and total SER. For dictyosomes, the Vv was lower in all regions of MII oocytes; for SER-SV, the Vv was higher in all regions of MII oocytes; for SER-MV, the Vv was higher in all regions of MII oocytes, although not significant in the oocyte subcortex; for SER-VLV, the Vv was lower in all regions of MII oocytes; for SER-IT, the Vv was higher in all regions of MII oocytes; and for total SER ($P < 0.001$), the Vv was higher in all regions of MII oocytes.

Comparing MI with MII oocytes (Table 4), no significant differences in the Vv were found in relation to dictyosomes (although not significant, the Vv was higher in MII oocytes in the subcortex and IC), lysosomes (except for a significantly lower Vv in the cortex of MII oocytes and a non-significant higher Vv in the IC), CV (although not significant, the Vv was higher in MII oocytes, except for a significantly lower Vv in the IC) and SER-LV (although not significant, the Vv was higher in MII oocytes). Significant differences in the Vv were observed regarding mitochondria, SER-SV, SER-MV, SER-IT, aSERT and total SER. The Vv of mitochondria, SER-IT and aSERT were significantly lower in MII oocytes only when evaluating the total oocyte, with all regions displaying non-significantly lower Vv in MII oocytes. The Vv of total SER was significantly higher when evaluating the total oocyte and IC of MII oocytes, with non-significantly higher Vv in the cortex and subcortex of MII oocytes. The Vv of SER-SV was significantly higher in all regions of MII oocytes. The Vv of SER-MV was significantly lower in the cortex and subcortex of MII oocytes, and not significantly lower in the IC of MII oocytes.

Considering all these quantitative data, a gradual increase in SER elements, as described in morphological studies (Sundström *et al.*, 1985; Nottola *et al.*, 2014) and a decrease in dictyosomes (Sathananthan, 2003; Sathananthan *et al.*, 2006), was noted specifically from GV to MI stages. However, an increase in CV was expected along with oocyte maturation, as well as in aSERT and mitochondria–SER complexes in the oocyte cortex (Nottola *et al.*, 2014), which was not observed. Therefore, the cytoplasm of the oocytes analyzed in this study exhibited both GV and MI features, implying that they contained an immature cytoplasm.

Although a stereological analysis of mature (nuclear and cytoplasmic) MII oocytes is in progress, we think that the presentation of this anomaly (discrepant nuclear and cytoplasmic maturation in MII donor oocytes) deserves anticipated publication due to its immediate clinical importance.

In conclusion, we describe a case of donor MII oocytes exhibiting nuclear maturity simultaneously with cytoplasmic immaturity. If used in a donor programme, these oocytes would not be

https://doi.org/10.1017/S0967199423000114 Published online by Cambridge University Press

Table 2. Comparison of the means of organelle relative volume (Vv) between MII oocyte regions: Vv (organelle, cortex), Vv (organelle, subcortex) and Vv (organelle, inner cytoplasm)

Organelle	Kruskal–Wallis test (*P*-value*)	Oocyte regions	Mann–Whitney *U*-test (*P*-value*)
Mi	0.677		
Di	0.317		
Ly	0.003	Cortex vs Subcortex (Vv 0.03 vs Vv 0)	0.310
		Cortex vs Inner Cytoplasm (Vv 0.03 vs Vv 0.54)	0.008
		Subcortex vs Inner Cytoplasm (Vv 0 vs Vv 0.54)	0.008
CV	0.002	Cortex vs Subcortex (Vv 1.3 vs Vv 0.16)	0.008
		Cortex vs Inner Cytoplasm (Vv 1.3 vs Vv 0)	0.008
		Subcortex vs Inner Cytoplasm (Vv 0.16 0vs Vv 0)	0.008
VZP	0.032	Cortex vs Subcortex (Vv 0.08 vs Vv 0)	0.151
		Cortex vs Inner Cytoplasm (Vv 0.08 vs Vv 0)	0.151
		Subcortex vs Inner Cytoplasm (Vv 0 vs Vv 0)	1.000
SV	0.677		
MV	0.102		
LV	0.009	Cortex vs Subcortex (Vv 0.12 vs Vv 0.01)	1.000
		Cortex vs Inner Cytoplasm (Vv 0.12 vs Vv 1.27)	0.032
		Subcortex vs Inner Cytoplasm (Vv 0.01 vs Vv 1.27)	0.008
VLV	0.368		
IT	0.336		
aSERT	0.980		
Total SER	0.468		

*Significance set at $P < 0.05$
Mi: mitochondria; Di: dictyosomes; Ly: lysosomes; CV: cortical vesicles; VZP: vesicles containing zona pellucida-like material; SER: smooth endoplasmic reticulum; SV: SER small vesicles; MV: SER medium vesicles; LV: SER large vesicles; VLV: SER very large vesicles; IT: SER isolated tubules; aSERT: SER tubular aggregates.
Note: Mann–Whitney *U*-test was performed when the Kruskal–Wallis test gave a significant *P*-value.

Table 3. Comparison of the means of organelle relative volume (Vv) per oocyte region (organelle, cortex), Vv (organelle, subcortex) and Vv (organelle, inner cytoplasm) between GV oocytes and MII oocytes

	Total oocyte			Oocyte cortex			Subcortex			Inner cytoplasm		
	Vv			Vv			Vv			Vv		
Organelle	GV**	MII	*P*-value*	GV**	MII	*P*-value*	GV**	MII	*P*-value*	GV**	MII	*P*-value*
Mi	6.3	5.49	1.000	3.6	5.66	0.073	6.0	5.79	0.876	7.2	5.33	0.048
Di	0.5	0.01	<0.001	0.4	0	0.003	0.6	0.01	0.018	0.6	0.018	0.003
Ly	0.2	0.33	0.924	0.1	0.03	0.755	0.1	0	0.268	0.3	0.54	0.149
CV	0.3	0.3	0.485	1.3	1.29	1.00	0.1	0.16	0.343	0.1	0	0.003
VZP	0.05	0.02	0.214	0.2	0.084	0.106	0.02	0	0.432	0	0	0.755
SV	2.5	8.84	<0.001	2.0	9.67	0.003	2.3	8.74	0.005	2.7	8.40	0.040
MV	0.2	2.01	<0.001	0.1	1.04	0.005	0.2	0.74	0.106	0.3	2.75	0.005
LV	0.2	0.79	0.294	0.07	0.12	0.343	0.1	0.012	0.018	0.2	1.27	0.268
VLV	6.9	0.30	<0.001	0.9	0	0.003	1.67	0	0.003	10.1	0.49	0.003
IT	3.2	7.16	<0.001	3.3	8.19	0.018	3.2	7.22	0.010	3.1	7.2	0.010
Total SER (without VLV)	6.1	26.8	<0.001	4.6	19.99	0.003	5.8	17.1	0.003	6.23	20.1	0.003

*Significance set at $P < 0.05$.
**Data are presented as: organelle relative volume (Vv) found in GV oocytes (from Pires-Luís *et al*., 2016), organelle Vv found in MII oocytes (from Table 1), and the *P*-value obtained after comparison between the GV-organelle Vv and the MII-organelle Vv.
GV: prophase I oocytes (germinal vesicle oocytes); MII: metaphase II oocytes.
Mi: mitochondria; Di: dictyosomes; Ly: lysosomes; CV: cortical vesicles; VZP: vesicles containing zona pellucida-like material; SER: smooth endoplasmic reticulum; SV: SER small vesicles; MV: SER medium vesicles; LV: SER large vesicles; VLV: SER very large vesicles; IT: SER isolated tubules.
Note: aSERT (SER tubular aggregates) not included as not found in GV oocytes.

https://doi.org/10.1017/S0967199423000114 Published online by Cambridge University Press

Table 4. Comparison of the means of organelle relative volume (Vv) per oocyte region (organelle, cortex), Vv (organelle, subcortex) and Vv (organelle, inner cytoplasm) between MI oocytes and MII oocytes

	Oocyte			Cortex			Subcortex			Inner cytoplasm		
	Vv			Vv			Vv			Vv		
Organelle	MI **	MII	*P*-value*	MI**	MII	*P*-value*	MI**	MII	*P*-value*	MI**	MII	*P*-value*
Mi	6.5	5.49	0.023	6.3	5.66	0.690	7.3	5.79	0.095	6.4	5.33	0.421
Di	0.01	0.01	0.713	0.01	0	0.310	0	0.01	0.690	0.01	0.018	1.000
Ly	0.4	0.3	0.074	0.3	0.03	0.032	0.3	0	0.151	0.4	0.54	1.000
CV	0.4	0.3	0.775	0.96	1.29	0.548	0.1	0.16	0.421	0.1	0	0.008
SV	0.2	8.84	<0.001	0.2	9.67	0.008	0.2	8.74	0.008	0.2	8.40	0.008
MV	4.5	2.0	0.001	4.1	1.04	0.032	3.5	0.74	0.016	4.7	2.75	0.421
LV	0.2	0.79	0.935	0.07	0.12	0.310	0	0.012	0.690	0.2	1.27	0.095
IT	9.4	7.2	<0.001	10.4	8.19	0.056	9.6	7.22	0.095	8.8	7.2	0.056
aSERT	0.8	0.3	0.008	1.02	0.98	0.151	1.3	0.38	0.222	0.6	0.44	0.151
Total SER	15.05	26.8	0.013	15.9	19.99	0.151	14.6	17.1	0.548	14.5	20.1	0.032

*Significance set at $P < 0.05$.
**Data are presented as: organelle relative volume (Vv) found in MI oocytes (from Coelho *et al.*, 2020), organelle Vv found in MII oocytes (from Table 1), and the *P*-value obtained after comparison between the MI-organelle Vv and the MII-organelle Vv.
Mi: mitochondria; Di: dictyosomes; Ly: lysosomes; CV: cortical vesicles; SER: smooth endoplasmic reticulum; SV: SER small vesicles; MV: SER medium vesicles; LV: SER large vesicles; IT: SER isolated tubules: aSERT: SER tubular aggregates.
Note: VZP (vesicles containing zona pellucida-like material) and VLV (SER very large vesicles) not included. as not found in MI oocytes.

fertilized, and therefore this finding is the first demonstration of a possible cause of ART failure in oocyte donor cycles, in which oocyte quality is usually taken for granted.

Ethics approval and consent to participate

The authors declare that they followed all rules of ethical conduct regarding originality, data processing and analysis, duplicate publication and biological material. All authors critically read the final manuscript and agreed with the author order.

Ethical guidelines were followed conducting the research. According to the National Law on Medically Assisted Procreation (Law 32/2006) and the National Council for Medically Assisted Procreation guidelines (2018), the use of clinical databases and surplus gametes for research may be used under strict individual anonymity and after patient written informed consent. Surplus donor oocytes were used after the patient signed an informed consent agreeing to share their own gamete samples for the present study. The present laboratorial experiments were executed under the Joint Ethics Committee of the Hospital and University, CHUP/ICBAS approval number 2019/CE/P017 (266/CETI/ ICBAS). This work did not involve human or animal experiments and therefore the provisions of the Declaration of Helsinki as revised in Tokyo 2004 do not apply.

Data availability statement. The authors confirm that the data supporting the findings of this study is available upon request.

Acknowledgements. Not applicable.

Author contributions. T.S. was responsible for the stereology and statistic work, data analysis, critical discussion, a draft of the manuscript and a critical review of the final manuscript. A.S.P.L. was responsible for study design, stereology and statistic training, electron microscopy image acquisition, data analysis, critical discussion and critical review of the final manuscript. A.A. and E.O. were responsible for oocyte processing to electron microscopy and critical review of the final manuscript. C.L. was responsible for the embryologic work, donor oocyte selection and critical review of the final manuscript. M.F. was responsible for the psychological evaluation of the donor and the critical review of the final manuscript. E.V.F. and M.B. were responsible for clinical donor selection, ovarian stimulation, oocyte retrieval and critical review of the final manuscript. A.M.C. was responsible for critical review of the final manuscript. R.S. was responsible for critical discussion and review of the final manuscript. M.S. was responsible for study conceptualization, electron microscopy image acquisition, data analysis, critical discussion and writing of the final manuscript. All authors have read and agreed to the order of appearance and the published version of the manuscript.

Funding. ICBAS-UP and UMIB/ITR. The UMIB-Unit for Multidisciplinary Research in Biomedicine is funded by the Foundation for Science and Technology (FCT) Portugal (grant numbers UIDB/00215/2020 and UIDP/00215/2020) and the ITR-Laboratory for Integrative and Translational Research in Population Health (LA/P/0064/2020).

Conflict of Interest. The authors declare that the research was conducted in the absence of any commercial or financial relationships that could be construed as a potential conflict of interest.

Institutional review board statement. Not applicable.

Informed consent statement. Not applicable

References

Arroyo, A., Kim, B. and Yeh, J. (2020). Luteinizing hormone action in human oocyte maturation and quality: Signaling pathways, regulation, and clinical impact. *Reproductive Sciences*, **27**(6), 1223–1252. doi: 10.1007/s43032-019-00137-x

Azevedo, A. R., Pinho, M. J., Silva, J., Sá, R., Thorsteinsdóttir, S., Barros, A. and Sousa, M. (2014). Molecular cytogenetics of human single pronucleated zygotes. *Reproductive Sciences*, **21**(12), 1472–1482. doi: 10.1177/1933719114530185

Baca, M. and Zamboni, L. (1967). The fine structure of human follicular oocytes. *Journal of Ultrastructure Research*, **19**(3), 354–381. doi: 10.1016/s0022-5320(67)80225-9

Braga, D. P. A. F., Setti, A. S., Figueira, R. C. S. F., Machado, R. B., Iaconelli, A. and Borges, E. (2013). Influence of oocyte dysmorphisms on blastocyst

formation and quality. *Fertility and Sterility*, **100**(3), 748–754. doi: 10.1016/j.fertnstert.2013.05.021

Braga, D. P. A. F., Zanetti, B. F., Setti, A. S., Iaconelli, A. and Borges, E. (2020). Immature oocyte incidence: Contributing factors and effects on mature sibling oocytes in intracytoplasmic sperm injection cycles. *JBRA Assisted Reproduction*, **24**(1), 70–76. doi: 10.5935/1518-0557.20190056

Canosa, S., Adriaenssens, T., Coucke, W., Dalmasso, P., Revelli, A., Benedetto, C. and Smitz, J. (2017). Zona pellucida gene mRNA expression in human oocytes is related to oocyte maturity, zona inner layer retardance and fertilization competence. *Molecular Human Reproduction*, **23**(5), 292–303. doi: 10.1093/molehr/gax008

Cillo, F., Brevini, T. A. L., Antonini, S., Paffoni, A., Ragni, G. and Gandolfi, F. (2007). Association between human oocyte developmental competence and expression levels of some cumulus genes. *Reproduction*, **134**(5), 645–650. doi: 10.1530/REP-07-0182

Coelho, S., Pires-Luís, A. S., Oliveira, E., Alves, Â., Leal, C., Cunha, M., Barreiro, M., Barros, A., Sá, R. and Sousa, M. (2020). Stereological study of organelle distribution in human oocytes at metaphase I. *Zygote*, **28**(4), 308–317. doi: 10.1017/S0967199420000131

Conselho nacional de procriação medicamente assistida. (2018). Requisitos e parâmetros de funcionamento dos centros de PMA. Available from https://www.cnpma.org.pt/profissionais/Documents/Profissionais_Requisitos_CentrosPMA_2018_.pdf

Conti, M. and Franciosi, F. (2018). Acquisition of oocyte competence to develop as an embryo: Integrated nuclear and cytoplasmic events. *Human Reproduction Update*, **24**(3), 245–266. doi: 10.1093/humupd/dmx040

Cornet-Bartolomé, D., Barragán, M., Zambelli, F., Ferrer-Vaquer, A., Tiscornia, G., Balcells, S., Rodriguez, A., Grinberg, D. and Vassena, R. (2021). Human oocyte meiotic maturation is associated with a specific profile of alternatively spliced transcript isoforms. *Molecular Reproduction and Development*, **88**(9), 605–617. doi: 10.1002/mrd.23526

Coticchio, G., Dal Canto, M., Mignini Renzini, M. M., Guglielmo, M. C., Brambillasca, F., Turchi, D., Novara, P. V. and Fadini, R. (2015). Oocyte maturation: Gamete-somatic cells interactions, meiotic resumption, cytoskeletal dynamics and cytoplasmic reorganization. *Human Reproduction Update*, **21**(4), 427–454. doi: 10.1093/humupd/dmv011

Coticchio, G., Ophir, L., Yung, Y., Baum, M., Dal Canto, M., Mignini-Renzini, M., Brambillasca, F., Fadini, R. and Hourvitz, A. (2017). Differential regulation of cumulus cell transcription during oocyte maturation *in vivo* and *in vitro*. *International Journal of Developmental Biology*, **61**(6–7), 433–437. doi: 10.1387/ijdb.160364gc

Dale, B., Wilding, M., Coppola, G. and Tosti, E. (2010). How do spermatozoa activate oocytes? *Reproductive Biomedicine Online*, **21**(1), 1–3. doi: 10.1016/j.rbmo.2010.02.015

De Vos, M., Grynberg, M., Ho, T. M., Yuan, Y., Albertini, D. F. and Gilchrist, R. B. (2021). Perspectives on the development and future of oocyte IVM in clinical practice. *Journal of Assisted Reproduction and Genetics*, **38**(6), 1265–1280. doi: 10.1007/s10815-021-02263-5

Dumesic, D. A., Meldrum, D. R., Katz-Jaffe, M. G., Krisher, R. L. and Schoolcraft, W. B. (2015). Oocyte environment: Follicular fluid and cumulus cells are critical for oocyte health. *Fertility and Sterility*, **103**(2), 303–316. doi: 10.1016/j.fertnstert.2014.11.015

Ebner, T., Moser, M., Sommergruber, M. and Tews, G. (2003). Selection based on morphological assessment of oocytes and embryos at different stages of preimplantation development: A review. *Human Reproduction Update*, **9**(3), 251–262. doi: 10.1093/humupd/dmg021

Ebner, T., Moser, M. and Tews, G. (2006). Is oocyte morphology prognostic of embryo developmental potential after ICSI? *Reproductive Biomedicine Online*, **12**(4), 507–512. doi: 10.1016/s1472-6483(10)62006-8

El-Shafie, M., Windt, M.-L., Kitshoff, M., McGregor, P., Sousa, M., Wranz, P. A. B. and Kruger, T. F. (2000). Ultrastructure of human oocytes: a transmission electron microscopy view. In: El-Shafie, M., Sousa, M. and Kruger, T. F. (eds). *An Atlas of the Ultrastructure of Human Oocytes: A Guide for Assisted Reproduction*. The Parthenon Publishing Group, NY, USA. pp. 82–173.

Eppig, J. J. (1996). Coordination of nuclear and cytoplasmic oocyte maturation in eutherian mammals. *Reproduction, Fertility, and Development*, **8**(4), 485–489. doi: 10.1071/RD9960485

European IVF-Monitoring Consortium (EIM) for the European Society of Human Reproduction and Embryology (ESHRE), Wyns, C., De Geyter, C., Calhaz-Jorge, C., Kupka, M. S., Motrenko, T., Smeenk, J., Bergh, C., Tandler-Schneider, A., Rugescu, I. A., Vidakovic, S. and Goossens, V. (2021). ART in Europe, 2017: Results generated from European registries by ESHRE. *Human Reproduction Open*, 2021(3), hoab026. doi: 10.1093/hropen/hoab026

Familiari, G., Heyn, R., Relucenti, M., Nottola, S. A. and Sathananthan, A. H. (2006). Ultrastructural dynamics of human reproduction, from ovulation to fertilization and early embryo development. *International Review of Cytology*, **249**, 53–141. doi: 10.1016/S0074-7696(06)49002-1

Gasca, S., Pellestor, F., Assou, S., Loup, V., Anahory, T., Dechaud, H., De Vos, J. and Hamamah, S. (2007). Identifying new human oocyte marker genes: A microarray approach. *Reproductive Biomedicine Online*, **14**(2), 175–183. doi: 10.1016/s1472-6483(10)60785-7

Hinduja, I. N., Kumar, A. and Anand Kumar, T. C. (1990). Ultrastructure of the cortex in the human egg. *Human Reproduction*, **5**(1), 66–70. doi: 10.1093/oxfordjournals.humrep.a137043

Huirne, J. A., Homburg, R. and Lambalk, C. B. (2007). Are GnRH antagonists comparable to agonists for use in IVF? *Human Reproduction*, **22**(11), 2805–2813. doi: 10.1093/humrep/dem270

Karavani, G., Wasserzug-Pash, P., Mordechai-Daniel, T., Bauman, D., Klutstein, M. and Imbar, T. (2021). Age-dependent *in vitro* maturation efficacy of human oocytes – Is there an optimal age? *Frontiers in Cell and Developmental Biology*, **9**, 667682. doi: 10.3389/fcell.2021.667682

Mao, L., Lou, H., Lou, Y., Wang, N. and Jin, F. (2014). Behaviour of cytoplasmic organelles and cytoskeleton during oocyte maturation. *Reproductive Biomedicine Online*, **28**(3), 284–299. doi: 10.1016/j.rbmo.2013.10.016

May-Panloup, P., Boucret, L., Chao de la Barca, J. M., Desquiret-Dumas, V., Ferré-L'Hotellier, V., Morinière, C., Descamps, P., Procaccio, V. and Reynier, P. (2016). Ovarian ageing: The role of mitochondria in oocytes and follicles. *Human Reproduction Update*, **22**(6), 725–743. doi: 10.1093/humupd/dmw028

Morimoto, Y. (2009). Ultrastructure of the human oocytes during *in vitro* maturation. *Journal of Mammalian Ova Research*, **26**(1), 10–17. https://doi.otg/40.1274/jmor.26.10. doi: 10.1274/jmor.26.10

Motta, P. M., Nottola, S. A., Makabe, S., Heyn, R. and Jansen, R. (2000). Mitochondrial morphology in human fetal and adult female germ cells. *Human Reproduction*, **15** (Suppl. 2), 129–147. doi: 10.1093/humrep/15.suppl_2.129

Motta, P. M., Nottola, S. A., Micara, G. and Familiari, G. (1988). Ultrastructure of human unfertilized oocytes and polyspermic embryos in an IVF-ET program. *Annals of the New York Academy of Sciences*, **541**, 367–383. doi: 10.1111/j.1749-6632.1988.tb22274.x

Nottola, S. A., Macchiarelli, G. and Familiari, G. (2014). Fine structural markers of human oocyte quality in assisted reproduction. *Austin Journal of Reproductive Medicine and Infertility*, **1**(1), 5. Available at https://austinpublishinggroup.com/reproductive-medicine/fulltext/ajrm-v1-id1002.pdf

Ouandaogo, Z. G., Frydman, N., Hesters, L., Assou, S., Haouzi, D., Dechaud, H., Frydman, R. and Hamamah, S. (2012). Differences in transcriptomic profiles of human cumulus cells isolated from oocytes at GV, MI and MII stages after *in vivo* and *in vitro* oocyte maturation. *Human Reproduction*, **27**(8), 2438–2447. doi: 10.1093/humrep/des172

Ozturk, S. (2020). Selection of competent oocytes by morphological criteria for assisted reproductive technologies. *Molecular Reproduction and Development*, **87**(10), 1021–1036. doi: 10.1002/mrd.23420

Pinto, F., Oliveira, C., Cardoso, M. F., Teixeira-da-Silva, J., Silva, J., Sousa, M. and Barros, A. (2009). Impact of GnRH ovarian stimulation protocols on intracytoplasmic sperm injection outcomes. *Reproductive Biology and Endocrinology: RB&E*, **7**, 5. doi: 10.1186/1477-7827-7-5

Pires-Luís, A. S., Rocha, E., Bartosch, C., Oliveira, E., Silva, J., Barros, A., Sá, R. and Sousa, M. (2016). A stereological study on organelle distribution in human oocytes at prophase I. *Zygote*, **24**(3), 346–354. doi: 10.1017/S0967199415000258

Reader, K. L., Stanton, J. L. and Juengel, J. L. (2017). The role of oocyte organelles in determining developmental competence. *Biology*, **6**(3), 35. doi: 10.3390/biology6030035

Richani, D. and Gilchrist, R. B. (2018). The epidermal growth factor network: Role in oocyte growth, maturation and developmental competence. *Human Reproduction Update*, **24**(1), 1–14. doi: 10.1093/humupd/dmx029

Rienzi, L., Vajta, G. and Ubaldi, F. (2011). Predictive value of oocyte morphology in human IVF: A systematic review of the literature. *Human Reproduction Update*, **17**(1), 34–45. doi: 10.1093/humupd/dmq029

Sá, R., Cunha, M., Silva, J., Luís, A., Oliveira, C., Teixeira da Silva, J., Barros, A. and Sousa, M. (2011). Ultrastructure of tubular smooth endoplasmic reticulum aggregates in human metaphase II oocytes and clinical implications. *Fertility and Sterility*, **96**(1), 143–149.e7. doi: 10.1016/j.fertnstert.2011.04.088

Sánchez, F. and Smitz, J. (2012). Molecular control of oogenesis. *Biochimica et Biophysica Acta*, **1822**(12), 1896–1912. doi: 10.1016/j.bbadis.2012.05.013

Sathananthan, A. H. (1985). Maturation of the human oocyte *in vitro*: Nuclear events during meiosis (an ultrastructural study). *Gamete Research*, **12**(3), 237–254. doi: 10.1002/mrd.1120120303

Sathananthan, A. H. (1994). Ultrastructural changes during meiotic maturation in mammalian oocytes: Unique aspects of the human oocyte. *Microscopy Research and Technique*, **27**(2), 145–164. doi: 10.1002/jemt.1070270208

Sathananthan, A. H. (1997). Ultrastructure of the human egg. *Human Cell*, **10**(1), 21–38.

Sathananthan, A. H. (2003). Morphology and pathology of the human oocyte. In: Trounson, A. O. and Gosden, R. G. (eds). *Biology and Pathology of the Oocyte* (1st edn), pp. 185–208. Cambridge University Press.

Sathananthan, A. H. (2013). Ultrastructure of human gametes, fertilization and embryos in assisted reproduction: A personal survey. *Micron*, **44**, 1–20. doi: 10.1016/j.micron.2012.05.002

Sathananthan, A. H. and Trounson, A. O. (1982). Ultrastructural observations on cortical granules in human follicular oocytes cultured *in vitro*. *Molecular Reproduction and Development*, **5**, 191–198. doi: 10.1002/mrd.112005o2o9

Sathananthan, A. H. and Trounson, A. O. (2000). Mitochondrial morphology during preimplantational human embryogenesis. *Human Reproduction*, **15** (Suppl. 2), 148–159. doi: 10.1093/humrep/15.suppl_2.148

Sathananthan, A. H., Selvaraj, K., Girijashankar, M. L., Ganesh, V., Selvaraj, P. and Trounson, A. O. (2006). From oogonia to mature oocytes: Inactivation of the maternal centrosome in humans. *Microscopy Research and Technique*, **69**(6), 396–407. doi: 10.1002/jemt.20299

Sciorio, R., Antonini, E. and Engl, B. (2021) Live birth and clinical outcome of vitrification-warming donor oocyte programme: An experience of a single IVF unit. *Zygote*, **29**(5), 410–416. doi: 10.1017/S0967199421000204

Setti, A. S., Braga, D. P. A. F., Iaconelli, A. and Borges, E. (2021). Fresh oocyte cycles yield improved embryo quality compared with frozen oocyte cycles in an egg-sharing donation programme. *Zygote*, **29**(3), 234–238. doi: 10.1017/S0967199420000842

Shen, X., Liu, X., Zhu, P., Zhang, Y., Wang, J., Wang, Y., Wang, W., Liu, J., Li, N. and Liu, F. (2017). Proteomic analysis of human follicular fluid associated with successful *in vitro* fertilization. *Reproductive Biology and Endocrinology: RB&E*, **15**(1), 58. doi: 10.1186/s12958-017-0277-y

Shu, Y., Gebhardt, J., Watt, J., Lyon, J., Dasig, D. and Behr, B. (2007). Fertilization, embryo development, and clinical outcome of immature oocytes from stimulated intracytoplasmic sperm injection cycles. *Fertility and Sterility*, **87**(5), 1022–1027. doi: 10.1016/J.FERTNSTERT.2006.08.110

Sirait, B., Wiweko, B., Jusuf, A. A., Iftitah, D. and Muharam, R. (2021). Oocyte competence biomarkers associated with oocyte maturation: A review. *Frontiers in Cell and Developmental Biology*, **9**(9), 710292. doi: 10.3389/fcell.2021.710292

Sousa, M. and Tesarik, J. (1994). Ultrastructural analysis of fertilization failure after intracytoplasmic sperm injection. *Human Reproduction*, **9**(12), 2374–2380. doi: 10.1093/oxfordjournals.humrep.a138455

Sousa, M., Barros, A. and Tesarik, J. (1996). Developmental changes in calcium dynamics, protein kinase C distribution and endoplasmic reticulum organization in human preimplantation embryos. *Molecular Human Reproduction*, **2**(12), 967–977. doi: 10.1093/molehr/2.12.967

Sousa, M., Barros, A., Silva, J. and Tesarik, J. (1997). Developmental changes in calcium content of ultrastructurally distinct subcellular compartments of preimplantation human embryos. *Molecular Human Reproduction*, **3**(2), 83–90. doi: 10.1093/molehr/3.2.83

Sousa, M., Teixeira da Silva, J., Silva, J., Cunha, M., Viana, P., Oliveira, E., Sá, R., Soares, C., Oliveira, C. and Barros, A. (2015). Embryological, clinical and ultrastructural study of human oocytes presenting indented zona pellucida. *Zygote*, **23**(1), 145–157. doi: 10.1017/S0967199413000403

Sousa, M., Cunha, M., Silva, J., Oliveira, E., Pinho, M. J., Almeida, C., Sá, R., da Silva, J. T., Oliveira, C. and Barros, A. (2016a). Ultrastructural and cytogenetic analyses of mature human oocyte dysmorphisms with respect to clinical outcomes. *Journal of Assisted Reproduction and Genetics*, **33**(8), 1041–1057. doi: 10.1007/s10815-016-0739-8

Sousa, M., Oliveira, E., Barros, N., Barros, A. and Sá, R. (2016b). New ultrastructural observations of human oocyte smooth endoplasmic reticulum tubular aggregates and cortical reaction: Update on the molecular mechanisms involved. *Revista Internacional de Andrología*, **14**(4), 113–122. doi: 10.1016/j.androl.2016.04.005

Stigliani, S., Moretti, S., Casciano, I., Canepa, P., Remorgida, V., Anserini, P. and Scaruffi, P. (2018). Presence of aggregates of smooth endoplasmic reticulum in MII oocytes affects oocyte competence: Molecular-based evidence. *Molecular Human Reproduction*, **24**(6), 310–317. doi: 10.1093/molehr/gay018

Sundström, P., Nilsson, B. O., Liedholm, P. and Larsson, E. (1985). Ultrastructure of maturing human oocytes. *Annals of the New York Academy of Sciences*, **442**, 324–331. doi: 10.1111/j.1749-6632.1985.tb37536.x

Taylor, A. (2019). Gamete donation. In: Stuart, J. A. (ed.), *Subfertility, Reproductive Endocrinology and Assisted Reproduction*, pp. 241–250. Cambridge University Press. doi: 10.1017/9781316488294.032

Ten, J., Mendiola, J., Vioque, J., de Juan, J. and Bernabeu, R. (2007). Donor oocyte dysmorphisms and their influence on fertilization and embryo quality. *Reproductive Biomedicine Online*, **14**(1), 40–48. doi: 10.1016/s1472-6483(10)60762-6

Trebichalská, Z., Kyjovská, D., Kloudová, S., Otevřel, P., Hampl, A. and Holubcová, Z. (2021). Cytoplasmic maturation in human oocytes: An ultrastructural study. *Biology of Reproduction*, **104**(1), 106–116. doi: 10.1093/BIOLRE/IOAA174

Tripathi, A., Kumar, K. V. and Chaube, S. K. (2010). Meiotic cell cycle arrest in mammalian oocytes. *Journal of Cellular Physiology*, **223**(3), 592–600. doi: 10.1002/jcp.22108

Venturas, M., Yang, X., Kumar, K., Wells, D., Racowsky, C. and Needleman, D. J. (2021). Metabolic imaging of human cumulus cells reveals associations among metabolic profiles of cumulus cells, patient clinical factors, and oocyte maturity. *Fertility and Sterility*, **116**(6), 1651–1662. doi: 10.1016/j.fertnstert.2021.07.1204

Virant-Klun, I., Leicht, S., Hughes, C. and Krijgsveld, J. (2016). Identification of maturation-specific proteins by single-cell proteomics of human oocytes. *Molecular and Cellular Proteomics*, **15**(8), 2616–2627. doi: 10.1074/mcp.M115.056887

Walker, M. H. and Tobler, K. J. (2022) Female Infertility. In: StatPearls [Internet]. Treasure Island (FL): StatPearls Publishing; 2022 Jan-. [Updated 2022 May 26] Available from: https://www.ncbi.nlm.nih.gov/books/NBK556033/

Watson, A. J. (2007). Oocyte cytoplasmic maturation: A key mediator of oocyte and embryo developmental competence. *Journal of Animal Science*, **85**(13) (Suppl.), E1–E3. doi: 10.2527/jas.2006-432

Weibel, E. R., Kistler, G. S. and Scherle, W. F. (1966). Practical stereological methods for morphometric cytology. *Journal of Cell Biology*, **30**(1), 23–38. doi: 10.1083/jcb.30.1.23

Wells, D. and Patrizio, P. (2008). Gene expression profiling of human oocytes at different maturational stages and after *in vitro* maturation. *American Journal of Obstetrics and Gynecology*, **198**(4), 455.e1–9; discussion 455.e9. doi: 10.1016/j.ajog.2007.12.030

Williams, R. S., Ellis, D. D., Wilkinson, E. A., Kramer, J. M., Datta, S. and Guzick, D. S. (2022). Factors affecting live birth rates in donor oocytes from commercial egg banks vs. program egg donors: An analysis of 40,485 cycles from the Society for Assisted Reproductive Technology registry in 2016–2018. *Fertility and Sterility*, **117**(2), 339–348. doi: 10.1016/j.fertnstert.2021.10.006

Windt, M. L., Coetzee, K., Kruger, T. F., Marino, H., Kitshoff, M. S. and Sousa, M. (2001). Ultrastructural evaluation of recurrent and in-vitro

maturation resistant metaphase I arrested oocytes. *Human Reproduction*, **16**(11), 2394–2398. doi: 10.1093/humrep/16.11.2394

World Health Organization. (2020). *Infertility*. Available from https://www.who.int/news-room/fact-sheets/detail/infertility

Yeh, J. S., Steward, R. G., Dude, A. M., Shah, A. A., Goldfarb, J. M. and Muasher, S. J. (2014). Pregnancy outcomes decline in recipients over age 44: an analysis of 27,959 fresh donor oocyte *in vitro* fertilization cycles from the Society for Assisted Reproductive Technology. *Fertility and Sterility*, **101**(5), 1331–1336.e1. doi: 10.1016/J.FERTNSTERT.2014.01.056

Zamboni, L., Thompson, R. S. and Smith, D. M. (1972). Fine morphology of human oocyte maturation *in vitro*. *Biology of Reproduction*, **7**(3), 425–457. doi: 10.1093/BIOLREPROD/7.3.425

https://doi.org/10.1017/S0967199423000114 Published online by Cambridge University Press